



## Asperochones A and B, two antimicrobial aromatic polyketides from the endophytic fungus *Aspergillus* sp. MMC-2

Hong Zhang<sup>1</sup>, Cui-Ping Li<sup>1</sup>, Li-Li Wang, Zhuo-Da Zhou, Wen-Sen Li, Ling-Yi Kong\*, Ming-Hua Yang\*

Jiangsu Key Laboratory of Bioactive Natural Product Research and State Key Laboratory of Natural Medicines, China Pharmaceutical University, Nanjing 210009, China

### ARTICLE INFO

#### Article history:

Received 7 October 2023  
Revised 23 November 2023  
Accepted 26 November 2023  
Available online 7 December 2023

#### Keywords:

*Aspergillus* sp.  
Asperochones A and B  
Aromatic polyketides  
Heterotrimeric compound  
Anti-tuberculosis effect  
Antifibrotic activity

### ABSTRACT

Two novel fungal metabolites, asperochones A and B, were obtained from an *Aspergillus* sp. Their structures were determined by 1D/2D nuclear magnetic resonance (NMR) spectroscopy, high resolution electrospray ionization mass spectroscopy (HRESIMS), and single-crystal X-ray diffraction analysis. Asperochone A possesses an intriguing skeleton bearing 5/6/6/6/7/5/5/5 octacyclic ring system, and asperochone B also exhibits an unusual carbon skeleton with five stereochiral centers. Their structures were proposed as heterotrimeric and heterodimeric products of aromatic polyketides. In addition, asperochone A exhibited a potential anti-tuberculosis effect since it showed a moderate potency against *Mycobacterium smegmatis*.

© 2024 Published by Elsevier B.V. on behalf of Chinese Chemical Society and Institute of Materia Medica, Chinese Academy of Medical Sciences.

Using a succinct suite of chemical reactions, nature is adept at orchestrating the assembly of rudimentary building blocks into a vast array of secondary metabolites. These metabolites can sometimes assemble even more complex natural products through a series of intricate polyreactions, such as lignans and tannins from plants [1–6]. Besides the secondary metabolites from the plant kingdom, metabolites derived from fungi also exhibit substantial structural diversity. In recent years, numerous polymeric products have been reported with intriguing structural attributes and notable bioactivities. Aspercholasine A, isolated from *Aspergillus flavipes*, serves as a quintessential example [7]. Its complex molecular scaffold is generated by the fusion of two cytochalasins to an epcoccine, containing as many as 20 chiral centers. There are many other sophisticated polymeric metabolites, like stephacidin B, homodimericin A, distachydrimane F, and eupenifeldin [8–11]. These complexes are not only great resources of bioactive compounds but also treasure to learn the art of synthesis from nature.

*Aspergillus* spp. have immense biosynthetic potential of secondary metabolites. Over 3000 compounds including 343 polyketide derivatives had been discovered from *Aspergillus* strains by the end of 2022 [12–15]. These polyketides are categorized into numer-

ous types, with some experiencing further diversification through dimerization. The typical *Aspergillus*-derived dimers are dimeric naphthopyranones and anthraquinones, both of which had been found in different *Aspergillus* spp. [16–18]. Some other polymeric products are continuously being discovered in these years. For example, we uncovered several heterodimers of azaphilone and furanone from a symbiotic *Aspergillus* strain in 2017 [19]. Subsequently, two alkaloids featuring highly analogous tetracyclic skeletons were subsequently isolated last year from a sponge-derived *Aspergillus* sp., affirming that *Aspergillus* spp. continue to be promising reservoirs of complex and bioactive natural products [12]. In our ongoing search of antimicrobial compounds from endophytic fungi from *Pinellia ternata*, we found that the *Aspergillus* sp. MMC-2 strain had obvious antibacterial effect when coculturing with pathogenic bacteria. The subsequent isolation was resulted in two unique aromatic polyketides, asperochone A (**1**) and B (**2**). Compound **1** possesses an intriguing skeleton bearing 5/6/6/6/7/5/5/5 octacyclic ring system. Its oxepane ring (H) angularly fused to a 1,6-dioxaspiro[4.4]nonane structure (F and G rings), forming a “broken” [5.5.7]trioxafenestrane (Fig. 1). The [5.5.5.7]fenestrane is naturally rare but do exist as the diterpene laurenene, while the “broken” [5.5.7]fenestrane is only found in a few synthesis studies [20]. Compound **1** was proposed as a polymeric product of three aromatic polyketides, while compound **2** is a dimeric metabolite of the same precursors to **1**. In addition, compound **1** also showed moderate antimicrobial activity including anti-tuberculosis poten-

\* Corresponding authors.

E-mail addresses: [cpu\\_lykong@126.com](mailto:cpu_lykong@126.com) (L.-Y. Kong), [skeepjack@163.com](mailto:skeepjack@163.com) (M.-H. Yang).

<sup>1</sup> These authors contributed equally to this work.

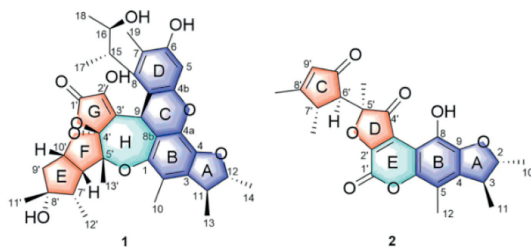


Fig. 1. Structures of asperochones A (1) and B (2).

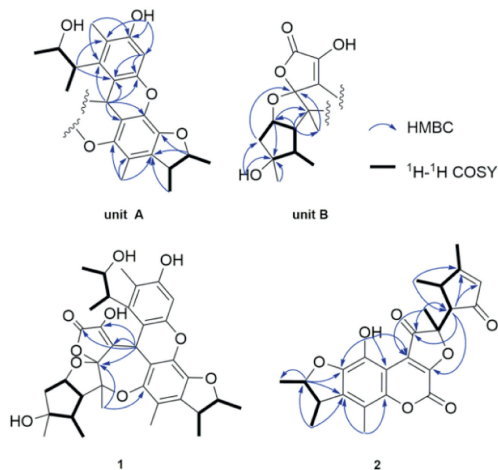


Fig. 2.  $^1\text{H}$ - $^1\text{H}$  COSY and key HMBC correlations of 1 and 2.

tial. Herein, we describe their structure determination, antimicrobial evaluation, and plausible biosynthetic pathways.

Asperochone A (**1**) was obtained as colorless crystals. The molecular formula of  $\text{C}_{36}\text{H}_{42}\text{O}_{10}$  was deduced from the molecular ion sodium adduct at  $m/z$  657.2670 [ $\text{M} + \text{Na}$ ] $^+$  (calcd. for  $\text{C}_{36}\text{H}_{42}\text{O}_{10}\text{Na}$ , 657.2673), corresponding to sixteen degrees of unsaturation. Its infrared spectroscopy (IR) spectrum suggested the presence of carbonyl ( $1777\text{ cm}^{-1}$ ), olefinic ( $1603\text{ cm}^{-1}$ ), and hydroxy ( $3435\text{ cm}^{-1}$ ) groups. The  $^1\text{H}$  nuclear magnetic resonance (NMR) spectrum (Table S1 in Supporting information) clearly displayed five secondary methyls ( $\delta_{\text{H}}$  1.39, 1.31, 1.23, 1.12, and 1.08), and four tertiary methyls ( $\delta_{\text{H}}$  2.24, 2.16, 1.16, and 1.11), and one aromatic proton ( $\delta_{\text{H}}$  6.42, 1H, s). Other protons, with the help of heteronuclear single quantum correlation (HSQC) spectrum, were assigned as one methylene ( $\delta_{\text{H}}$  2.01, d,  $J = 13.7\text{ Hz}$ ; 2.15, m), eight methines ( $\delta_{\text{H}}$  4.79, s; 3.09, m; 4.52, m; 3.32, m; 4.19, m; 3.16, t,  $J = 8.6\text{ Hz}$ ; 2.27, m; 4.84, td,  $J = 8.2, 1.8\text{ Hz}$ ), and two hydroxy protons ( $\delta_{\text{H}}$  9.45, 1H, s; 4.07, 1H, s). Apart from these proton-bearing carbons, there were still 17 non-proton-bearing carbons which were deduced as one carbonyl, thirteen aromatic, and three quaternary carbons according to their chemical shifts. All above functional groups accounted for eight unsaturation degrees. An octacyclic ring system was therefore indicated for **1**.

Structural details were revealed by the interpretation of 2D NMR spectra (Fig. 2). The 2,3,4-trimethyl-5,7-dihydroxy-2,3-dihydrobenzofuran fragment (rings A and B) was revealed by the  $^1\text{H}$ - $^1\text{H}$  correlation spectroscopy ( $^1\text{H}$ - $^1\text{H}$  COSY) cross-peaks of  $\text{H}_3$ -14/ $\text{H}$ -12/ $\text{H}$ -11/ $\text{H}_3$ -13 and the heteronuclear multiple-bond correlation spectroscopy (HMBC) correlations mainly from  $\text{H}_3$ -10 to C-1/C-2/C-3, from  $\text{H}_3$ -13 to C-3, and from H-12 to C-3/C-4 at first. The fragment of 3-(3-hydroxybutan-2-ol)-2-methylphenol (ring D) was then determined by the  $^1\text{H}$ - $^1\text{H}$  COSY cross-peaks of  $\text{H}_3$ -18/ $\text{H}$ -16/ $\text{H}$ -15/ $\text{H}_3$ -17 along with the HMBC correlations from H-15 to C-7 and C-8a, from OH-6 to C-5/C-6/C-7, from  $\text{H}_3$ -19 to C-6/C-7/C-8,

and from H-5 to C-6/C-7/C-4b/C-8a. The key proton at  $\delta_{\text{H}}$  4.79 (H-9) showed HMBC correlations with C-1, C-4a, C-8b, C-8, C-8a, and C-4b, which thus indicated a 9H-xantheno structure (unit A) for **1**.

In the  $^1\text{H}$ - $^1\text{H}$  COSY spectrum, interpretation starting from the methyl at  $\delta_{\text{H}}$  1.39 (d,  $J = 7.4\text{ Hz}$ , H-12') revealed another spin system from C-12' to C-9' as shown in Fig. 2, which, combined with the HMBC correlations from  $\text{H}_3$ -11' to C-7'/C-8'/C-9' and from H-9' and H-10' to C-8', undoubtedly revealed a dimethyl-substituted cyclopentane fragment (ring E). An additional hydroxyl was substituted on C-8' since its broad singlet ( $\delta_{\text{H}}$  4.07) showed HMBC correlations with C-7'/C-8'/C-9'. Meantime, according to the HMBC correlations from H-6' to C-5'/C-10'/C-13', from  $\text{H}_3$ -13' to C-4'/C-5'/C-6', from H-10' to C-5'/C-6', and from  $\text{H}_2$ -9' to C-4', a methyl-substituted tetrahydrofuran ring (ring F) was fused to the cyclopentane through C-6' and C-10'. Hereto, there were still three non-proton-bearing carbons at  $\delta_{\text{C}}$  166.9 (C-1'), 131.9 (C-2'), and 126.0 (C-3'). Judged from their chemical shifts [21,22], the ketal nature of C-4' (116.1), and three unattributed oxygen atoms left, a  $\beta$ -hydroxy-substituted  $\alpha,\beta$ -unsaturated- $\gamma$ -lactone (ring G) were hypothetically connected to the tetrahydrofuran ring via C-4' to form a 1,6-dioxaspiro[4,4]nonane structure (unit B). Between two structural units, the C9-C3' bond was established through the HMBC correlations from H-9 to C-2', C-3', and C-4'. Another connection, the C-5'-O-C-1 ether linkage, was deduced from the long-range correlation from  $\text{H}_3$ -13' to C-1, which further formed the oxepane ring (ring H) between the two units. The planar structure was thus determined (Fig. 2).

In the rotating-frame overhauser effect spectroscopy (ROESY) spectrum, the correlations from H-7' to H-10' and  $\text{H}_3$ -11' and from H-6' to  $\text{H}_3$ -13' and H-10' indicated the same orientation that was randomly assigned as  $\beta$  configurations. H-9 was assigned for an  $\alpha$ -orientation by its nuclear Overhauser effect (NOE) correlations with OH-8', which along with the determined  $\beta$  configuration of H-10' revealed that the lactone ring G was closely approximated in space with H-6' and H-10'. Additionally,  $\text{H}_3$ -13 and H-12 were determined as  $\beta$  orientation since ROESY correlations were obtained from  $\text{H}_3$ -13 to  $\text{H}_3$ -13' and H-12 and from H-11 to  $\text{H}_3$ -14. The 3-hydroxy-2-butyl chain at C-8 was deduced in an *erythro* configuration by the empirical chemical shift rules of 18- $\text{CH}_3$  ( $\delta_{\text{C}}$  17.1) and 17- $\text{CH}_3$  ( $\delta_{\text{C}}$  22.8) [23]. A single-crystal X-ray diffraction experiment, using the anomalous scattering of Cu  $K\alpha$  radiation (the Flack parameter of 0.05, CCDC 2124874), subsequently confirmed the above structural determination and revealed the absolute configuration as 9S, 11S, 12R, 15S, 16R, 4'S, 5'R, 6'R, 7'S, 8'R, and 10'S (Fig. 3).

Asperochone B (**2**) was obtained as reddish crystals. Its molecular formula  $\text{C}_{24}\text{H}_{24}\text{O}_7$  was determined by the positive HRESIMS ion peak at  $m/z$  447.1415 [ $\text{M} + \text{Na}$ ] $^+$  (calcd. for  $\text{C}_{24}\text{H}_{24}\text{O}_7\text{Na}$ , 447.1414), indicating 13 degrees of unsaturation. The  $^1\text{H}$  NMR spectrum (Table S2 in Supporting information) of **2** obviously exhibited six methyls ( $\delta_{\text{H}}$  1.35, 1.45, 2.34, 2.18, 1.43, and 1.71) and one olefinic methine ( $\delta_{\text{H}}$  5.87), and the other four methines were recognized by HSQC spectrum. The 13 carbons left were all non-proton-bearing

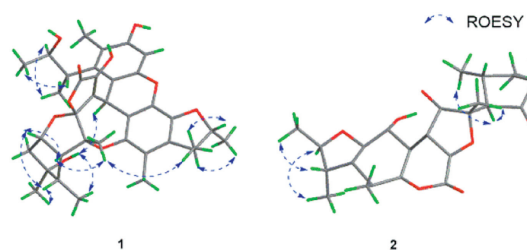


Fig. 3. Key ROESY correlations of 1 and 2.

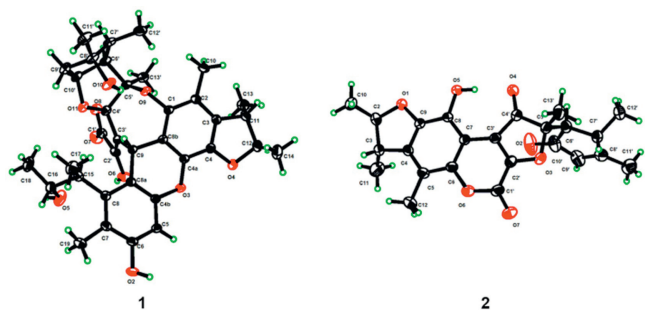


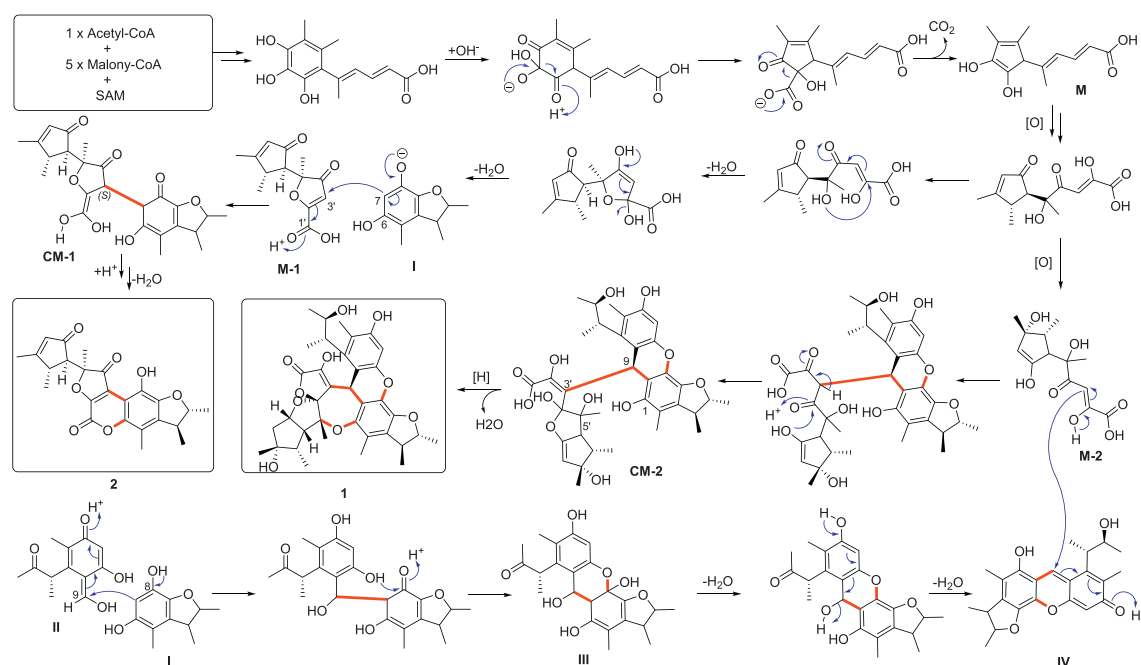
Fig. 4. X-ray crystallographic structures of **1** and **2**.

ones which were distinguished as three carbonyl, six aromatic, three olefinic, and one quaternary carbon. By analyzing 2D NMR data, the dihydrobenzofuran fragment (rings A and B) like that in **1** was easily determined for **2** according to those key correlations as shown in Fig. 2. Another fragment easy to determine was the spin system from H<sub>3</sub>-12' to H-6' as shown by <sup>1</sup>H-<sup>1</sup>H COSY correlations. Since HMBC cross-peaks were observed from H-6' to C-8'/C-9'/C-10' and from H-9' to C-6'/C-8'/C-10'/C-11', the 5-ethyl-3,4-dimethylcyclopent-2-en-1-one ring C was thus established. The furan-3(2H)-one ring D that was linked at C-6' was further established by the HMBC correlations from H<sub>3</sub>-13' to C-3'/C-4'/C-5' and from H-6' to C-4'/C-2'. The C7-C3' linkage between rings B and D was deduced by the weak HMBC correlation from OH-8 (δ<sub>H</sub> 9.82) to C-3'. Thus far there still was one carbonyl (δ<sub>C</sub> 158.8) left without any useful 2D NMR correlations. Its high-field chemical shift and the remained one degree of unsaturation however led to the unsaturated lactone ring E. As for its configuration, the opposite orientations of H-2/H-3 and of H-6'/H-7' were indicated by the ROESY correlations of H-2/H<sub>3</sub>-11, H-3/H<sub>3</sub>-10, and H-6'/H<sub>3</sub>-12', while the observable NOE effects were unable to settle the relative configuration of H<sub>3</sub>-13' (Fig. 3). The single-crystal X-ray diffraction of **2** [Flack parameter 0.04 (8), CCDC 2125429] was therefore carried out and established the structure and its configuration (Fig. 4).

As shown in Scheme 1, **M** is a key precursor in the hypothetical biosynthetic pathways of both **1** and **2**. However, to the best of our knowledge, there are no fungal metabolites analogous to **M** identified thus far. Terrein is the most resembled one [27]. Since its cyclopentane is derived from an aromatic ring through oxidative cleavage, we deduced a similar process involving oxidation and decarboxylation to obtain **M** [24–28]. It further underwent a series of oxidation and dehydration to yield **M-1** [29,30]. In the meantime, intermediate **I**, a known product from *Aspergillus* spp. [31,32], contributed a nucleophilic carbanion intermediate through deprotonating its 8-OH. Michael addition thereafter yielded **CM-1** which converted to **2** by esterification between 2'-COOH and 6-OH [4,30,33]. Compound **1** is a heterotrimeric product. Its monomeric precursor **M-2** was deduced from a biosynthetic pathway like **M-1**. 8-Enol-keto tautomerism induced electron addition to C-9 of intermediate **II**, a quinoid form of the precursor of decarboxycitrinin, followed by cyclization and dehydration to deliver **III**. Intermediate **III** further derived **IV** from continuous dehydration. The adduct **CM-2** was subsequently generated by intermolecular nucleophilic addition between **IV** and **M-2**, which finally turned into **1** after cyclization, dehydration, and reduction.

Compound **1** showed potential anti-tuberculosis activity since it totally inhibited the growth of *Mycobacterium smegmatis* at 80 μg/mL (Fig. 5). Compound **1** also demonstrated inhibitory activity against *Staphylococcus aureus*, *Bacillus subtilis*, and *Pseudomonas aeruginosa* with the concentration that inhibited growth of 50% of isolates (MIC<sub>50</sub>) values of 9.4 ± 0.9, 6.4 ± 0.7, and 2.5 ± 1.0 μg/mL respectively (Table S3 in Supporting information). Compound **2** was inactive against pathogenic bacteria tested. Additionally, they were also evaluated for *in vitro* antifibrotic activity. Compound **1** (20 μmol/L) was significantly suppressed the transforming growth factor β1 (TGF-β1)-induced expression of *COL1A1* and *ACTA2* in LX-2 cells (Fig. S1 in Supporting information) [34,35].

In conclusion, we have isolated two unprecedented fungal metabolites, each exemplifying a distinctive carbon skeleton. They are presumed to be polymeric products of aromatic polyketides, and a series of tailoring enzymes and potential nonenzymatic re-



Scheme 1. Hypothetical biosynthetic pathways for **1** and **2**.

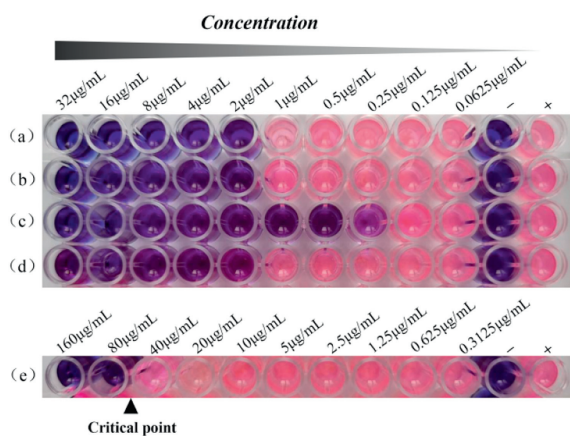


**Fig. 5.** Drug susceptibility of compound **1** (e) against *M. smegmatis* by resazurin method. Rifampin (a), kanamycin (b), atreptomycin (c), and isoniazid (d) are positive controls. Sterile medium with no bacteria or drug (–) and medium contain bacteria, but no drug (+) are growth controls ( $n = 3$ ).

actions could be involved in their biosynthetic pathways. This research further substantiates the statement that fungi are sophisticated in assembling diverse building blocks, yielding metabolites with chemical and biological diversity.

#### Declaration of competing interest

The authors declare that they have no known competing financial interests or personal relationships that could have appeared to influence the work reported in this paper.

#### Acknowledgments

This study was supported by the National Natural Science Foundation of China (No. 32170403), the 111 Center from Ministry of Education of China and the State Administration of Foreign Experts Affairs of China (No. B18056), the “Double First-Class” University Project (No. CPU2018GF03), and the Drug Innovation Major Project (Nos. 2018ZX09711-001-007 and 2018ZX09735002-003).

#### Supplementary materials

Supplementary material associated with this article can be found, in the online version, at doi:10.1016/j.ccllet.2023.109351.

#### References

- [1] P. Luo, Y.F. Cheng, Z.Y. Yin, et al., *J. Nat. Prod.* 82 (2019) 349–357.
- [2] J.E. Sears, D.L. Boger, *Acc. Chem. Res.* 48 (2015) 653–662.
- [3] X.P. Peng, G. Li, L.M. Wang, et al., *Front. Microbiol.* 13 (2022) 800626.
- [4] J.W. Liu, A.A. Liu, Y.C. Hu, *Nat. Prod. Rep.* 38 (2021) 1469–1505.
- [5] X.Z. Qi, J.B. Liu, J.B. Chen, et al., *Chin. Chem. Lett.* 31 (2020) 423–426.
- [6] L.J. Meng, Q.L. Guo, M.H. Chen, et al., *Chin. Chem. Lett.* 29 (2018) 1257–1260.
- [7] H.C. Zhu, C.M. Chen, Y.B. Xue, et al., *Angew. Chem. Int. Ed.* 54 (2015) 13374–13378.
- [8] J. Qian-Cutrone, S. Huang, Y.Z. Shu, et al., *J. Am. Chem. Soc.* 124 (2002) 14556–14557.
- [9] E. Mevers, J. Sauri, Y.Z. Liu, et al., *J. Am. Chem. Soc.* 138 (2016) 12324–12327.
- [10] C. Schotte, L. Li, D. Wibberg, et al., *Angew. Chem. Int. Ed.* 59 (2020) 23870–23878.
- [11] S. Lin, J. Huang, H. Zeng, et al., *Chin. Chem. Lett.* 33 (2022) 4587–4594.
- [12] Y. Liu, L.J. Ding, Y.T. Shi, et al., *ACS Omega* 7 (2022) 9909–9916.
- [13] H.H. Li, Y.Q. Fu, F.H. Song, *Mar. Drugs* 21 (2023) 277–283.
- [14] X.L. Bai, Y. Sheng, Z.X. Tang, et al., *J. Fungi* 9 (2023) 261–284.
- [15] J. He, C.L. Xie, T.Z. Wu, et al., *Bioorg. Chem.* 139 (2023) 106756.
- [16] C.D. Donner, *Nat. Prod. Rep.* 32 (2015) 578–604.
- [17] M. Kawaguchi, T. Ohshiro, M. Toyoda, et al., *Angew. Chem. Int. Ed.* 57 (2018) 5115–5119.
- [18] S.H. Ghoran, F. Taktaz, S.A. Ayatollahi, et al., *Mar. Drugs* 20 (2022) 474–542.
- [19] G.P. Yin, Y.R. Wu, M.H. Yang, et al., *Org. Lett.* 19 (2017) 4058–4061.
- [20] A. Boudhar, M. Charpenay, G. Blond, et al., *Angew. Chem. Int. Ed.* 52 (2013) 12786–12798.
- [21] S.R.M. Ibrahim, G.A. Mohamed, S.A. Ross, *Z. Naturforsch. C* 72 (2017) 155–160.
- [22] M. Zhou, J. Lou, Y.K. Li, et al., *J. Braz. Chem. Soc.* 26 (2015) 545–549.
- [23] Z.Y. Lu, Z.J. Lin, W.L. Wang, et al., *J. Nat. Prod.* 71 (2008) 543–546.
- [24] C. Sommer-Kamann, A. Fries, S. Mordhorst, et al., *Angew. Chem. Int. Ed.* 56 (2017) 4033–4036.
- [25] X.Q. Xie, C. Khosla, D.E. Cane, *J. Am. Chem. Soc.* 139 (2017) 6102–6105.
- [26] M.E. Raggatt, T.J. Simpson, M.E. Raggatt, et al., *Chem. Commun.* (1997) 2245–2247.
- [27] L. Kahlert, D. Bernardi, M. Hauser, et al., *Chem. Eur. J.* 27 (2021) 11895–11903.
- [28] X. Shu, G.Z. Wei, Y.B. Qiao, et al., *Org. Lett.* 23 (2021) 8947–8951.
- [29] G.D. Chen, D. Hu, M.J. Huang, et al., *Chem. Commun.* 56 (2020) 4607–4610.
- [30] Y. Araki, T. Awakawa, M. Matsuzaki, et al., *Proc. Natl. Acad. Sci. U. S. A.* 116 (2019) 8269–8274.
- [31] Y. He, R.J. Cox, *Chem. Sci.* 7 (2016) 2119–2127.
- [32] B.R. Clark, R.J. Capon, E. Lacey, et al., *Org. Biomol. Chem.* 4 (2006) 1520–1528.
- [33] X.D. Jiang, Z.J. Fang, Q.B. Zhang, et al., *Org. Biomol. Chem.* 19 (2021) 4243–4247.
- [34] D.J. Xiang, J. Zou, X.Y. Zhu, et al., *Phytomedicine* 78 (2020) 153294.
- [35] I. Lua, D. James, J.H. Wang, et al., *Hepatology* 60 (2014) 311–322.